Rapid glucose sensing by protein kinase A for insulin exocytosis in mouse pancreatic islets

Hiroyasu Hatakeyama

DOCTOR OF PHILOSOPHY

Department of Physiological Sciences

School of Life Science

The Graduate University for Advanced Studies

2005

Contents

Summary **2**

Introduction **3**

Methods **6**
Isolation of mouse pancreatic islets and islet cell clusters 6
TEP imaging 7
Photolysis of NPE and Ca^{2+} measurements 9
Statistical analysis 10

Results **11**
Role of PKA in the first phase of glucose-induced insulin exocytosis 11
Rapid effects of glucose and PKA on Ca^{2+}-induced insulin exocytosis 19
Control of the fusion pore by PKA 24

Discussion **28**
Role of the basal activity of PKA in glucose-induced insulin exocytosis 28
The PKA-dependent mechanism of glucose sensing 29

Acknowledgements **35**

References **36**

Summary

The role of protein kinase A (PKA) in insulin exocytosis was investigated with the use of two-photon excitation imaging of mouse islets of Langerhans. Inhibitors of PKA selectively reduced the number of exocytic events during the initial period (< 250 s) of the first phase of glucose-induced exocytosis (GIE), without affecting the second phase, in intact islets or small clusters of islet cells. The PKA inhibitors did not reduce the extent of the glucose-induced increase in $[Ca^{2+}]_i$. The actions of glucose and PKA in Ca^{2+}-induced insulin exocytosis (CIE) triggered by photolysis of a caged-Ca^{2+} compound, which resulted in large increases in $[Ca^{2+}]_i$ and thereby bypassed the ATP-sensitive K^+ channel-dependent mechanism of glucose sensing, were therefore studied. A high concentration (20 mM) of glucose potentiated CIE within 1 min, and this effect was blocked by inhibitors of PKA. This PKA-dependent action of glucose required glucose metabolism, given that increasing the intracellular concentration of cAMP by treatment with forskolin potentiated CIE only at the high glucose concentration. Finally, PKA appeared to reduce the frequency of 'kiss-and-run' exocytic events and to promote full-fusion events during GIE. These data indicate that a PKA-dependent mechanism of glucose sensing, which is operative even at the basal level of PKA activity, plays an important role specifically in the first phase of GIE, and they suggest that the action of PKA is mediated at the level of the fusion reaction.

Introduction

Glucose is the most important physiological regulator of insulin secretion from β cells of islets of Langerhans. Islet β cells rapidly take up and metabolize glucose, resulting in an increase in the cytosolic concentration of ATP within 1 min (Bennett *et al.*, 1996; Porterfield *et al.*, 2000). Such increases in ATP concentration induce the closure of ATP-sensitive K^+ (K_{ATP}) channels and consequent depolarization of the cell membrane, again within a few minutes of glucose application (Henquin, 1990). Depolarization of the cell membrane to a voltage of > –50 mV results in activation of voltage-dependent Ca^{2+} channels and an increase in $[Ca^{2+}]_i$ that triggers insulin exocytosis. The K_{ATP} channels and Ca^{2+}-dependent mechanism are thought to play a central role in glucose sensing for insulin exocytosis. Although additional mechanisms of glucose sensing have been proposed to coexist (Gembal *et al.*, 1993; Aizawa *et al.*, 1994; Kasai *et al.*, 2002), their relative importance has remained unclear.

Exocytosis in many secretory cell types and neurons is regulated by both Ca^{2+} and cAMP (Wollheim & Sharp, 1981; Trudeau *et al.*, 1996; Renstrom *et al.*, 1997; Fujita-Yoshigaki *et al.*, 1999; Hilfiker *et al.*, 2001; Sato *et al.*, 2002; Sakaba & Neher, 2003; Kaneko & Takahashi, 2004). Our research group has previously shown that cytosolic cAMP potentiates Ca^{2+}-dependent insulin exocytosis (CIE) in β cells (Takahashi *et al.*, 1999). In these studies, individual β cells were subjected to whole-cell patch clamping and stimulated with large increases in $[Ca^{2+}]_i$ induced by photolysis of a caged-Ca^{2+} compound, thereby bypassing the K_{ATP} channel-dependent mechanism. We found that CIE was

augmented by cAMP in a manner dependent on protein kinase A (PKA) and cytosolic ATP. It was not possible to study the action of extracellular glucose under the whole-cell clamp conditions, however, and it has remained unknown whether PKA contributes to glucose-induced insulin exocytosis (GIE). Inhibitors of PKA have been shown to have relatively small inhibitory effects on GIE in previous studies, in which exocytosis was measured over a long period without separation into the first and second phases (Persaud *et al.*, 1990; Harris *et al.*, 1997).

We therefore subsequently developed an approach based on two-photon excitation imaging to quantify insulin exocytosis in intact pancreatic islets (Takahashi *et al.*, 2002a). This approach has been designated TEP (two-photon extracellular polar-tracer) imaging and TEPIQ (TEP imaging-based quantification) analysis (Kasai *et al.*, 2005). TEP imaging is able to monitor reliably and with a relatively high time resolution (< 1 s) individual insulin exocytic events in intact islet preparations and also allows analysis of the dynamics of the fusion pore that mediates exocytosis. We have previously applied this methodology to study GIE as well as CIE evoked by photolysis of a caged-Ca^{2+} compound (Takahashi *et al.*, 2004). With the use of this approach, I have now shown that a PKA-dependent mechanism, operative at the basal level of PKA activity, is important for the initial period of the first phase of GIE in mouse pancreatic islets. Furthermore, I found that PKA mediates rapid enhancement of CIE in islets only in the presence of high glucose concentration, indicating that PKA plays a glucose sensing role, specifically in the first phase of GIE. Given that the first phase of GIE is reduced in many individuals with type 2 diabetes

mellitus from an early stage of the disease (Vaag *et al.*, 1995), impairment of this mechanism may contribute to the pathogenesis of this condition.

Methods

Isolation of mouse pancreatic islets and islet cell clusters

Eight- to 12-week-old ICR mice were killed by cervical dislocation and pancreatic islets were isolated by collagenase digestion. Islets were maintained for 1–12 h under a humidified atmosphere of 5% CO_2 at 37°C in Dulbecco's modified Eagle's medium containing glucose (1.0 mg ml^{-1}) and supplemented with 10% fetal bovine serum, penicillin (100 μU ml^{-1}), and streptomycin (100 mg ml^{-1}). They were then transferred with a Pipetman (Gilson, Middleton, WI) to thin (0.1 mm) glass coverslips (Matsunami-glass, Osaka, Japan) in the recording chamber. The standard external bathing solution (Sol A) contained 150 mM NaCl, 5 mM KCl, 1 mM $MgCl_2$, 2 mM $CaCl_2$, 10 mM Hepes-NaOH (pH 7.4), and 2.8 mM glucose at 310 mosmol l^{-1}. A solution containing 20 mM glucose was prepared from Sol A by adjusting the osmolarity with deionized water to 310 mosmol l^{-1}. Imaging experiments were performed within 20 min after placing an islet in Sol A containing 0.7 mM sulforhodamine B (SRB; Molecular Probes, Eugene, OR) with or without 1.5 mM 10-kDa fluorescein dextran (FD; Molecular Probes). Islet cell clusters were prepared by triturating islets with a glass pipette and were plated directly onto the glass-bottomed recording chamber. Forskolin (Sigma, St. Louis, MO), cerulenin (Sigma), bisindolylmaleimide I (Calbiochem, La Jolla, CA), KN-62 (Seikagaku, Tokyo, Japan), ML-9 (Calbiochem), KT5720 (Calbiochem), and H89 (Sigma) were initially dissolved in DMSO at 10–50 mM and subsequently diluted in Sol A. Myristoylated PKA inhibitor amide 14–22 (PKI; Calbiochem), the Rp isomer of adenosine 3',5'-monophosphorothioate (Rp-cAMPS; Sigma), and

8-(4-chloro-phenylthio)-2'-*O*-methyladenosine-3',5'-monophosphate (8-CPT-2'-*O*-Me-cAMP; Biolog, Bremen, Germany) were dissolved directly in Sol A.

TEP imaging

Two-photon excitation imaging of islets was performed with an inverted microscope (IX70; Olympus, Tokyo, Japan) and a laser-scanning microscope (FluoView, Olympus) equipped with a water-immersion objective lens (UplanApo60xW/IR; NA, 1.2), as previously described (Liu *et al.*, 2005; Kishimoto *et al.*, 2005; Kasai *et al.*, 2005). The laser power at the specimen was 3–10 mW, and two-photon excitation was effected at 830 nm, with images acquired every 0.3–2 s. The fluorescence of SRB and that of fura-2, fura-2FF, or fura-4F were measured at 570–650 nm and at 400–550 nm, respectively. Twelve-bit images were color-coded with fall color codes of FluoView. All experimental procedures were performed under illumination with yellow light (FL40S-Y-F; National, Tokyo, Japan) to prevent unintentional photolysis of the caged-Ca^{2+} compound. Experiments were performed at room temperature (24–25°C).

The number of exocytic events was expressed per cell per minute on the basis of the following procedures. Exocytic events were counted in a region of interest (ROI) with an area of 3000–5000 μm^2. An individual ROI in islets contained many (10–40) cells, sectioned at various distances from their equatorial planes, and therefore included all cell aspects (bottom, top, and side views) (Takahashi *et al.*, 2002a). I counted the number of exocytic events

whose fluorescence intensity was > 20% of the maximal value; these events would be expected to occur within 1 μm from the focal plane, given the axial resolution of 1.4 μm of our setup (Kasai *et al.*, 2005). The thickness of the image for detection of exocytosis was therefore ~2 μm along the *z*-axis. This value was slightly modified from our previous studies (Takahashi *et al.*, 2002a; Takahashi *et al.*, 2004). Each area of 4000 μm^2 thus represented a total cell volume of 8000 μm^3, which corresponds to the volume of five β cells, if I assume a cell diameter of 14 μm and that β cells constitute 90% of islet cells. On the basis on this calculation (1 β cell per 800 μm^2), I converted the number of events per ROI to events per cell. Moreover, I express the rate of insulin exocytosis as $cell^{-1}$ min^{-1} to allow comparison between GIE and CIE. For the mean values of GIE in Table 1, the total events were measured between 0 and 250 s after the onset of high-glucose application and were divided by 2 min, given that the increase in $[Ca^{2+}]_i$ occurred with a lag of about 100–150 s (Table 2). For the mean values of CIE in Table 3, the total events were measured between 0 and 15 s after the onset of UV irradiation and were divided by 0.25 min.

My data were consistent with the notion that TEP imaging visualized all the exocytic events in the ROI (Takahashi *et al.*, 2002a; Kasai *et al.*, 2005). The measured rate of GIE of 6.4 vesicles $cell^{-1}$ min^{-1} (Table 1) corresponds to 12 vesicles $cell^{-1}$ min^{-1} at the higher temperature of 35ºC (Takahashi *et al.*, 2004). If I assume that a single insulin granule contains 2.6 fg of insulin (Hutton, 1989) and that an islet with a diameter of 200 μm contains 2600 β cells, the rate of insulin secretion at 35°C is predicted to be 82 pg per islet per minute, which is similar to the value of 67 pg per islet per minute obtained for mouse islets by

radioimmunoassay (Eto *et al.*, 1999).

Photolysis of NPE and Ca^{2+} measurement

The acetoxymethyl ester (AM) forms of fura-2 (Molecular Probes), fura-4F (Molecular Probes), and fura-2FF (Tef Laboratory, Austin, TX) as well as that of *o*-nitrophenyl-EGTA (NPE; Molecular Probes) were dissolved in DMSO at a concentration of 2–10 mM. Islets were loaded with these compounds by incubation for 30 min at 37°C in serum-free Dulbecco's modified Eagle's medium containing 10 μM fura-2-AM (or fura-4F-AM or fura-2FF-AM), 25 μM NPE-AM, 0.03% cremphor EL (Sigma), and 0.1% bovine serum albumin; they were then washed with Sol A. Photolysis of NPE was induced by brief irradiation (0.2–0.5 s) with a mercury lamp (IX-RFC, Olympus) 1 min after switching the glucose concentration of the extracellular solution. In some experiments, I monitored $[Ca^{2+}]_i$ simultaneously during this prephotolysis period.

Glucose-induced increases in $[Ca^{2+}]_i$ were measured with either fura-2 or fura-4F, whose K_d values are 0.18 and 1.16 μM, respectively (Wokosin *et al.*, 2004). I estimated F_{min}/F_{max} (minimal/maximal fluorescence intensity ratio) for fura-2 and fura-4F to be 0.3 and 0.46, respectively, in islet cells loaded with the corresponding AM forms. I expressed increases in $[Ca^{2+}]_i$ by the ratio $(F_0 - F)/F_0$ (Takahashi *et al.*, 2002a), where F_0 and F represent the fluorescence intensities of the dye before and after glucose stimulation, respectively. If I assume the resting $[Ca^{2+}]_i$ to be 0.1 μM, the ratio for fura-4F of ~0.3 predicted the peak $[Ca^{2+}]_i$ during glucose stimulation to be 1.8 μM. Increases in $[Ca^{2+}]_i$ induced by uncaging of NPE were monitored as the decrease in fluorescence

intensity of fura-2FF and were calculated as $K_d \frac{1 - F/F_{max}}{F/F_{max} - F_{min}/F_{max}}$. *In vivo* calibration of fura-2FF was performed as described (Takahashi *et al.*, 2004); I estimated F_{min}/F_{max} to be 0.1 and K_d is 31 μM. I assumed that the resting fluorescence was the same as F_{max}.

Statistical analysis

Data are presented as means ± S.E.M. Those in Tables 1 and 2 were compared by the one-way Kruskal–Wallis test and those in Table 3 by the two-way Friedman test; further comparisons between two conditions were performed by the Mann–Whitney *U* test, as indicated. Data in Table 4 were compared by the chi-square test. A *P*-value of < 0.05 was considered statistically significant. Statistical tests were performed with SPSS 12.0 software (SPSS, Chicago, IL).

Results

Role of PKA in the first phase of glucose-induced insulin exocytosis

I first examined the participation of PKA in GIE with the use of TEP imaging, in which insulin exocytic events were visualized by two-photon imaging of islets immersed in an extracellular solution containing the polar fluorescent tracer SRB at a concentration of 0.7 mM (see Fig. 4*A*) (Takahashi *et al.*, 2002a). I imaged mostly the outer second or third layer of cells in the islets because insulin-secreting β cells were abundant in these layers. I detected exocytic events as discrete spots of fluorescence, which reflected diffusion of SRB into individual insulin granules via the fusion pore (Takahashi *et al.*, 2002a). The intensities of the spots of SRB fluorescence were consistent with them reflecting exocytosis of large dense-core vesicles (Kasai *et al.*, 2005).

Islets were pretreated with either of two inhibitors of PKA, Rp-cAMPS or PKI (Harris *et al.*, 1997), for 40 min and insulin secretion was then stimulated with 20 mM glucose. Figure 1*A* shows the time courses of averaged exocytic events (cell^{-1} min^{-1}), with insulin exocytosis first being apparent 1–3 min after the onset of high-glucose application. Rp-cAMPS and PKI each markedly inhibited the initial period (< 250 s) of the first phase of GIE (< 7 min) (Nesher & Cerasi, 2002), with the number of exocytic events within this initial period being reduced in the presence of these agents to one-third or one-half of the control value, respectively (Table 1). The remaining period of the first phase and the second phase of GIE (250–600 s after stimulation) were not affected by Rp-cAMPS (control, 5.3 ± 0.86 events cell^{-1} min^{-1}, n = 9; Rp-cAMPS, 4.14 ± 1.53 events

cell^{-1} min^{-1}, n = 6, P > 0.1). In contrast, forskolin, which increases the cytosolic concentration of cAMP by activating adenylyl cyclase, increased the extent of secretion both during the first phase of GIE (Table 1) and during the second phase (11.8 ± 0.8 events cell^{-1} min^{-1}, n = 3, P < 0.05), consistent with previous observations (Takahashi *et al.*, 2002a). These data thus suggested that the initial period of the first phase of GIE, but not the second phase, requires PKA.

In contrast to the effects of Rp-cAMPS and PKI, one of the most widely used inhibitors of PKA, H89 (10–20 μM), did not markedly reduce the extent of GIE in intact islets (Fig. 1*B* and Table 1). Another inhibitor of PKA, KT5720 (1–5 μM) (Matthies & Reymann, 1993), was similarly ineffective in most of the islets examined (Fig. 1*B* and Table 1). I noticed, however, that the effects of both H89 and KT5720 were variable, tending to be more pronounced in smaller islets (data not shown), suggesting that their inability to inhibit GIE might be due to their poor penetration into islets. The AM form of the Ca^{2+} indicator fura-2 is similarly inefficient in its penetration into islets (Takahashi *et al.*, 2002b), with intense staining being limited to the outermost layer of cells.

I therefore tested the effects of H89 and KT5720 in cluster preparations of islets, which consist of groups of only 10–15 cells and would thus be expected to be more accessible to these lipophilic agents (Fig. 2*A*). Pretreatment of the cluster preparations with H89 or KT5720 resulted in marked inhibition of the first phase of GIE (Fig. 2*B* and Table 1), with the inhibitory effects again appearing more prominent during the initial period of this phase. Treatment of the clusters with forskolin also greatly increased the extent of the first phase of secretion in a manner sensitive to H89 or KT5720 (Fig. 2*C* and Table 1). These results thus

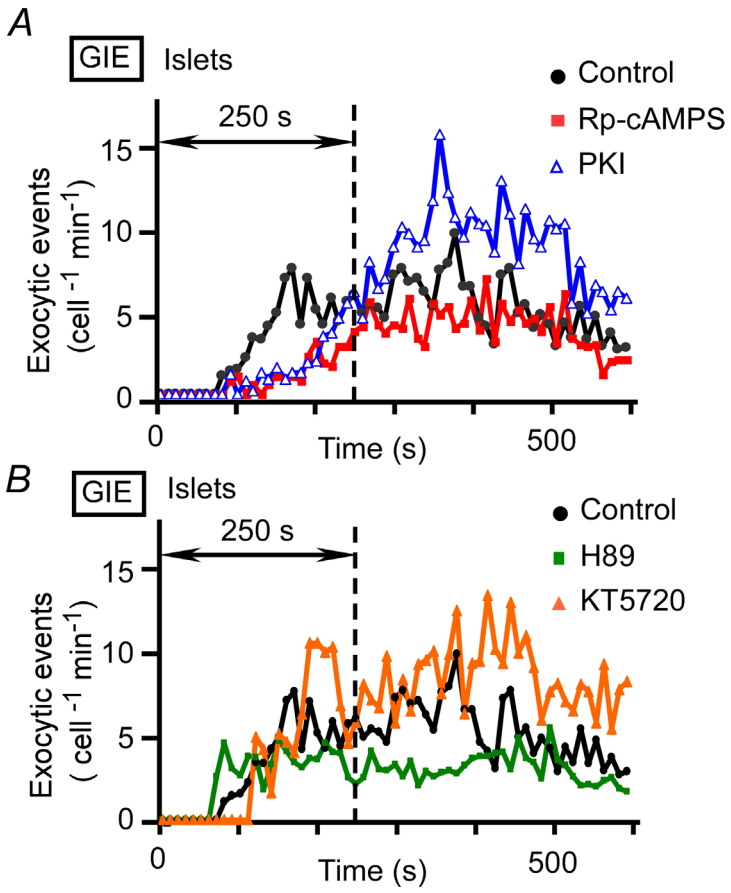

Figure 1. Effects of PKA inhibitors on GIE in mouse pancreatic islets

A, time courses of exocytic events in islets pretreated (or not) with Rp-cAMPS (200 μM) or PKI (5 μM) for 40 min and then stimulated with 20 mM glucose at time 0. *B*, time courses of exocytic events in islets pretreated (or not) with H89 (10–20 μM) or KT5720 (1–5 μM) for 40 min and then stimulated with 20 mM glucose at time 0. Data in *A* and *B* are expressed as the number of exocytic events per cell per minute and are averages from 3–10 islets, as indicated in Table 1. The bin width is 10 s, and the vertical dotted line indicates 250 s after the onset of stimulation with glucose.

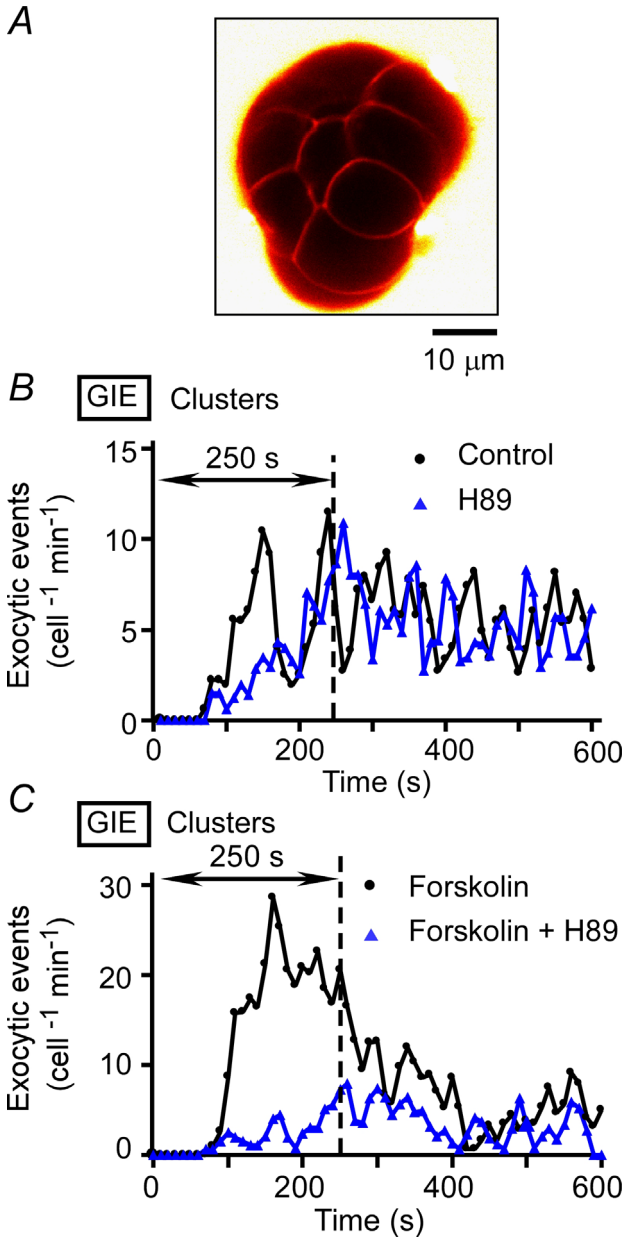

Figure 2. GIE in cluster preparations of mouse islet cells

A, a cluster preparation consisting of 10–15 islet cells. The cluster is visualized by SRB fluorescence. *B*, time courses of exocytic events in cluster preparations pretreated (or not) with 20 μM H89 for 40 min and then stimulated with 20 mM glucose at time 0. *C*, Time courses of exocytic events in cluster preparations pretreated (or not) with 20 μM H89 for 40 min and with 2 μM forskolin for 10 min and then stimulated with 20 mM glucose. Data in *B* and *C* are averages from three or four clusters, as indicated in Table 1.

Table 1. Pharmacology of the initial period (0–250 s) of glucose-induced insulin exocytosis (GIE) in intact islets or clusters of islet cells.

Preparation	Test agent (μM)	Events cell^{-1} min^{-1}	Significance
Islets	Control	6.4 ± 0.8 (9)	
	Rp-cAMPS (200)	2.0 ± 0.5 (8)	$P < 0.001$
	PKI (5)	3.1 ± 0.6 (9)	$P < 0.05$
	H89 (10-20)	6.4 ± 2.0 (10)	NS ($P = 0.66$)
	KT5720 (1–5)	7.0 ± 1.4 (3)	NS ($P = 0.73$)
	Forskolin (2)	13.8 ± 3.9 (3)	$P < 0.05$
Clusters	Control	8.9 ± 0.9 (4)	
	H89 (20)	5.0 ± 0.7 (4)	$P < 0.05$
	KT5720 (5)	1.0 ± 0.2 (4)	$P < 0.05$
	Forskolin (2)	25.2 ± 3.0 (3)	$P < 0.05$
	Forskolin (2) + H89 (20)	3.8 ± 0.8 (4)	*$P < 0.05$
	Forskolin (2) + KT5720 (5)	1.5 ± 0.4 (4)	*$P < 0.05$

Islets or cell clusters were pretreated (or not) for 40 min with PKA inhibitors or for 10 min with forskolin and were then stimulated with 20 mM glucose, as indicated. Data are means ± S.E.M. of values for the number of islets or islet cell clusters indicated in parentheses. Statistical analysis was performed with the Kruskal–Wallis test for all values ($P < 0.01$) followed by the Mann–Whitney *U* test for comparison with control values or, in the case of the *P* values indicated by an asterisk, with the corresponding value for forskolin.

provided further support for the notion that PKA is required for the initial period of the first phase of GIE.

I also measured the possible effects of PKA inhibitors and forskolin on glucose-induced increases in $[Ca^{2+}]_i$ in islets. Increases in $[Ca^{2+}]_i$ were measured with either the high-affinity Ca^{2+} indicator fura-2 (K_d = 0.18 μM) (Fig. 3*A*) or the low-affinity Ca^{2+} indicator fura-4F (K_d = 1.16 μM) (Fig. 3*B*); the latter was used in case fura-2 became saturated during the physiological increases in $[Ca^{2+}]_i$ (Ito *et al.*, 1999). Indeed, the fractional change in the fluorescence of fura-2 during glucose stimulation of islets was ~0.63 (Table 2), which is close to the saturation level of ~0.7 for cells loaded with fura-2-AM (Nemoto *et al.*, 2001), whereas the corresponding fractional change in the fluorescence of fura-4F was ~0.3 (Table 2). I found that neither the onset (measured by fura-2) nor the maximal value apparent within 250 s (measured by fura-4F) of the glucose-induced increases in $[Ca^{2+}]_i$ was affected by forskolin, Rp-cAMPS, or PKI (Fig. 3 and Table 2).

These results are consistent with previous observations that cAMP has only a small (if any) effect on glucose-induced increases in $[Ca^{2+}]_i$ in islets (Rorsman & Abrahamsson, 1985; Hill *et al.*, 1987; Fournier *et al.*, 1994; Marie & Bailbe, 2000). PKA has been found to modulate $[Ca^{2+}]_i$ by affecting voltage-gated Ca^{2+} channels (Grapengiesser *et al.*, 1991; Yada *et al.*, 1993; Yaekura *et al.*, 1996), Ca^{2+}-induced Ca^{2+} release (Bugrim, 1999; Dyachok & Gylfe, 2004; Kang *et al.*, 2005), or Ca^{2+} sequestration (Yaekura & Yada, 1998). Such effects were not evident, however, during glucose-induced increases in $[Ca^{2+}]_i$ under my experimental conditions and could not account for the action of PKA in GIE.

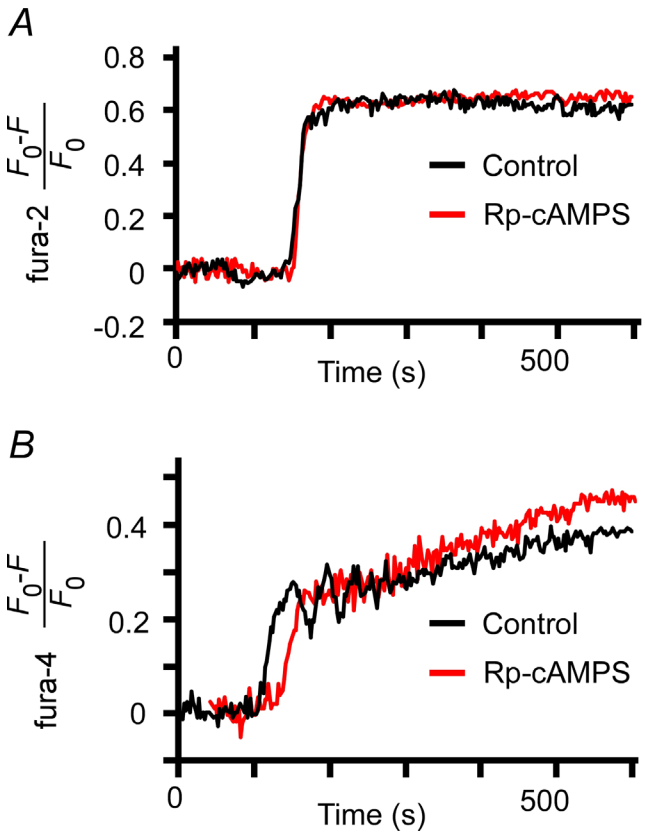

Figure 3. Increases in $[Ca^{2+}]_i$ during GIE

Time courses of glucose-induced increases in the fura-2 (*A*) or fura-4F (*B*) fluorescence ratio were determined for β cells in islets pretreated (or not) for 40 min with 200 μM Rp-cAMPS before stimulation with 20 mM glucose at time 0.

Table 2. Glucose-induced increases in $[Ca^{2+}]_i$ estimated with the Ca^{2+} indicators fura-2 or fura-4F

	Fura-2		Fura-4F
Condition	Latency (s)	$(F_0 - F)/F_0$	$(F_0 - F)/F_0$
Control	152.4 ± 5.6 (5)	0.63 ± 0.01 (5)	0.25 ± 0.05 (5)
Forskolin (2 μM)	121.3 ± 8.3 (4)	0.60 ± 0.02 (4)	0.33 ± 0.05 (3)
Rp-cAMPS (200 μM)	113.1 ± 23.2 (5)	0.67 ± 0.01 (5)	0.31 ± 0.02 (5)
PKI (20 μM)	104.9 ± 13.9 (5)	0.62 ± 0.03 (5)	
Kruskal–Wallis test	NS (P = 0.078)	NS (P = 0.10)	NS (P = 0.48)

Islets were pretreated (or not) for 40 min with PKA inhibitors or for 10 min with forskolin and were then stimulated with 20 mM glucose. Latencies were measured as the time between the onset of glucose stimulation and that of the fura-2 signal. The peak amplitudes of the fluorescence signals, $(F_0 - F)/F_0$, were obtained within 250 s after the onset of glucose stimulation for both indicators. Data are means ± S.E.M. for the number of cells indicated in parentheses. Statistical comparisons were performed with the Kruskal–Wallis test.

Rapid effects of glucose and PKA on Ca^{2+}-induced insulin exocytosis

I next examined whether glucose and PKA might directly potentiate CIE. For these experiments, Ca^{2+}-dependent mechanisms were saturated by large increases in $[Ca^{2+}]_i$ generated by photolysis of the caged-Ca^{2+} compound NPE, which was loaded into the cells of islets in the AM form. Exocytic events were detected as discrete spots of SRB fluorescence (Fig. 4*A*), as was the case with glucose stimulation (Takahashi *et al.*, 2002a). I confirmed that irradiation with UV light induced an abrupt increase in $[Ca^{2+}]_i$ of > 20 μM (Fig. 4*B*). The latency histogram for the discrete exocytic events was fitted by a probability density function with two exponential components (Fig. 4*C*), consistent with the characteristics of CIE studied by amperometry (Takahashi *et al.*, 1997; Takahashi *et al.*, 1999). The second component in the present study was smaller than that detected previously, however, probably as a result of the more rapid recovery of $[Ca^{2+}]_i$ (Fig. 4*B*) compared with that apparent in cells subjected to whole-cell dialysis (Takahashi *et al.*, 1997; Takahashi *et al.*, 1999). It was therefore difficult to compare the effects of glucose on the two components separately, and I counted all exocytic events between 0 and 15 s after the uncaging of NPE for the data shown in Table 3.

Exposure of islets to a high glucose concentration (20 mM) resulted in a marked increase in the extent of CIE (Fig. 4*C* and Table 3). This facilitatory effect was apparent at a glucose concentration as low as 8 mM (107 ± 25 events $cell^{-1}$ min^{-1}, $n = 6$, $P < 0.05$). Islets were exposed to high glucose for only 1 min before uncaging of NPE, during which time glucose alone did not increase $[Ca^{2+}]_i$ (Fig. 3 and Table 2). I confirmed that the high-glucose solution did not affect the

increase in $[Ca^{2+}]_i$ induced by uncaging of NPE (Fig. 4*B*). Also the glucose action was not mimicked by 2-deoxy-D-glucose (20 mM) (61.5 ± 5.6 $cell^{-1}$ min^{-1}, n = 5, P = 0.069), indicating that it required a metabolite of glucose.

The effect of glucose on CIE was abolished by pretreatment of islets (for 40 min) with inhibitors of PKA, including Rp-cAMPS and PKI (Fig. 5*A* and Table 3). Furthermore, forskolin did not significantly affect CIE at the low glucose concentration of 2.8 mM (Table 3) but potentiated the effect of 20 mM glucose on CIE (Fig. 5*B* and Table 3). These results suggested that cAMP is necessary but not sufficient for the rapid effect of glucose on CIE, and that a metabolite of glucose, such as ATP, is required for this action of glucose (see Discussion).

The effect of glucose on CIE was mediated largely by PKA. Indeed, PKI eliminated the effect of high glucose even in the presence of forskolin (Table 3). The effect of cAMP on insulin exocytosis has been proposed to be mediated also by cAMP-regulated guanine nucleotide exchange factor II (cAMP-GEFII) (Ozaki *et al.*, 2000). I therefore examined the possible role of this protein in my system with the use of 8-CPT-2′-*O*-Me-cAMP, which selectively activates cAMP-GEFII at 10 μM but also activates PKA at higher concentrations (Enserink *et al.*, 2002). CIE was not affected by 8-CPT-2′-*O*-Me-cAMP at 10 μM in the presence of low or high glucose, but it was slightly facilitated by this analog at 100 μM in the presence of high glucose (Table 3), similar to the effect of forskolin. The effect of 20 mM glucose plus 100 μM 8-CPT-2′-*O*-Me-cAMP was abolished by PKI (Table 3).

I also examined the possible roles of three other protein kinases (protein kinase C, calmodulin-dependent protein kinase II, and myosin light chain kinase)

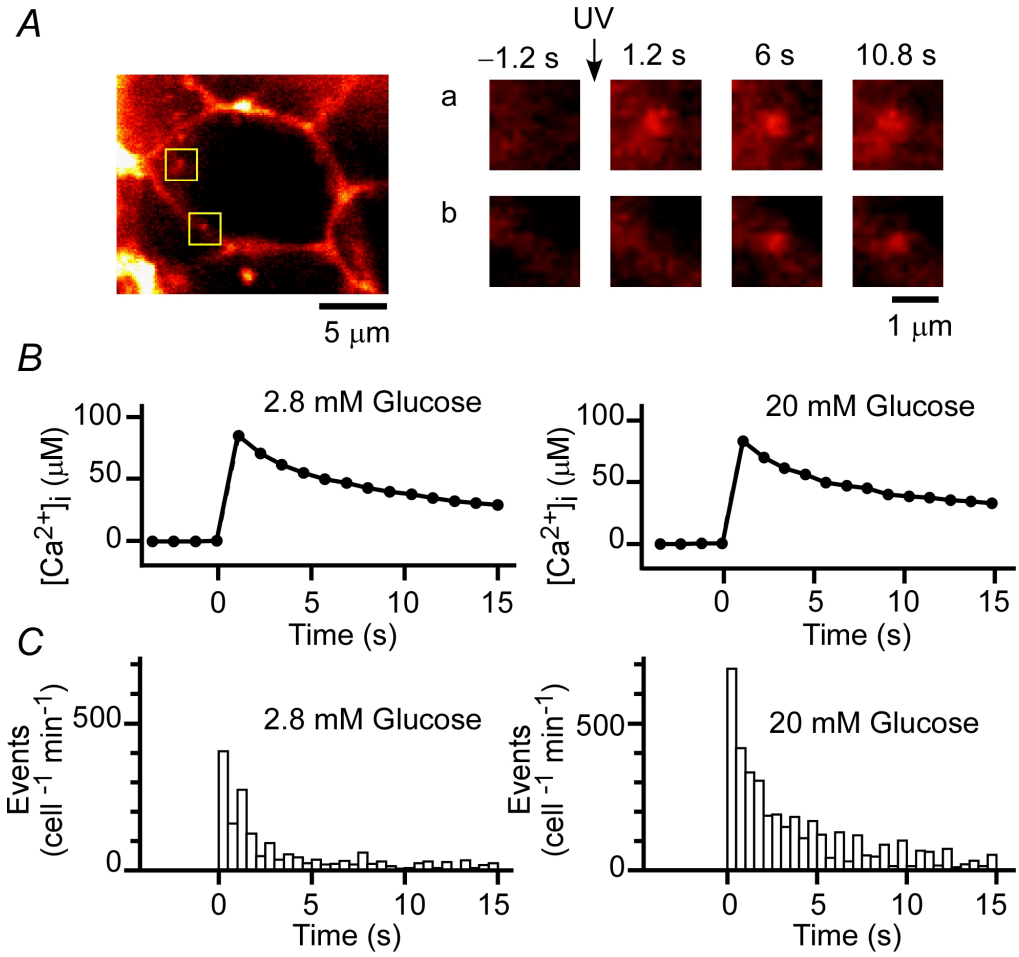

Figure 4. Effect of glucose on exocytosis induced by uncaging of a caged-Ca^{2+} compound in islets

A, insulin exocytosis in a β cell within an islet loaded with NPE and perifused with a solution containing SRB. Exocytosis was triggered by UV-induced photolysis of NPE at time 0. The boxed regions a and b in the micrograph on the left are sites of individual exocytic events after UV irradiation and are shown at higher magnification on the right. *B*, increases in $[Ca^{2+}]_i$ induced by uncaging of NPE at time 0 in islets loaded with the Ca^{2+} indicator fura-2FF and exposed to glucose at 2.8 or 20 mM. The high-glucose solution was applied 1 min before UV irradiation. Traces represent average time courses obtained from four to six islets. *C*, latency histograms of insulin exocytosis induced by uncaging of NPE (CIE) in islets exposed to glucose at 2.8 or 20 mM. The bin width is 0.5 s, and data are averages from nine and six islets, respectively, as indicated in Table 3.

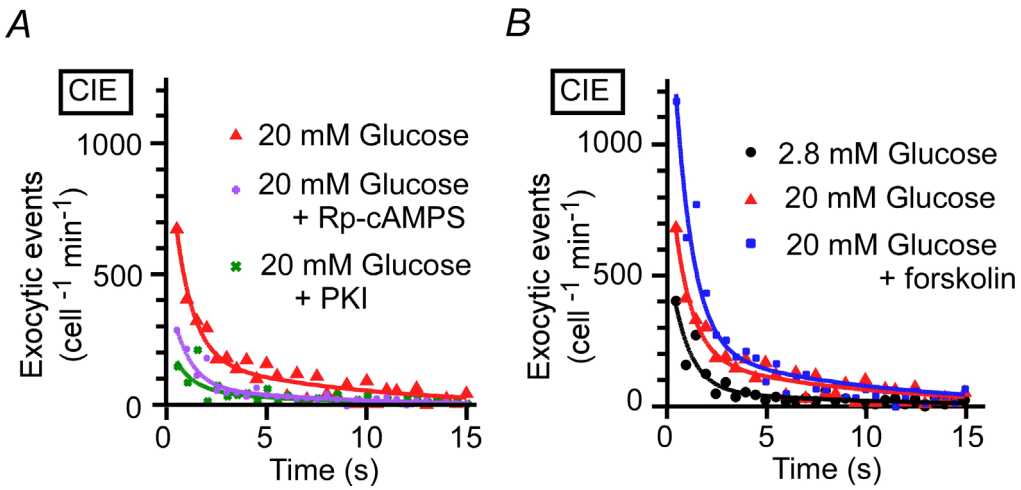

Figure 5. Insulin exocytosis induced by uncaging of NPE (CIE) in islets exposed to high glucose, PKA inhibitors, or forskolin

Rp-cAMPS or PKI was applied for 40 min (*A*), forskolin for 10 min (*B*), and high glucose for 1 min (*A*, *B*) before UV irradiation. Smooth lines are double-exponential curves, and the bin width is 0.5 s. Data are averages from five to nine islets, as indicated in Table 3.

Table 3. Pharmacology of Ca^{2+}-dependent insulin exocytosis (CIE)

Test agent (μM)	CIE (events $cell^{-1}$ min^{-1}) 2.8 mM Glucose	20 mM Glucose	Significance between 2.8 and 20 mM glucose
Control	68.1 ± 13.7 (9)	128.4 ± 11.6 (6)	$P < 0.05$
Rp-cAMPS (200)	44.5 ± 11.4 (4) NS ($P = 0.40$)	40.4 ± 3.6 (6) $P < 0.01$	NS ($P = 0.76$)
PKI (5)	52.6 ± 6.3 (4) NS ($P = 0.70$)	55.8 ± 10.7 (6) $P < 0.01$	NS ($P = 0.76$)
Forskolin (2)	82.8 ± 8.9 (5) NS ($P = 0.42$)	182.5 ± 16.9 (5) $P < 0.05$	$P < 0.01$
Forskolin (2) + PKI (5)	48.6 ± 4.5 (5) NS ($P = 0.51$)	67.0 ± 7.2 (5) $P < 0.01$	NS ($P = 0.22$)
8-CPT-2'-*O*-Me-cAMP (10)	70.5 ± 5.3 (7) NS ($P = 0.40$)	131.3 ± 8.7 (7) NS ($P = 0.94$)	$P < 0.001$
8-CPT-2'-*O*-Me-cAMP (100)	94.3 ± 7.1 (4) NS ($P = 0.14$)	159.3 ± 11.7 (4) $P < 0.05$	$P < 0.05$
8-CPT-2'-*O*-Me-cAMP (100) + PKI (5)	50.7 ± 4.4 (4) NS ($P = 0.82$)	80.2 ± 13.8 (4) $P < 0.05$	NS ($P = 0.11$)
Bisindolylmaleimide I (1)	58.0 ± 10.2 (3) NS ($P = 0.85$)	142.5 ± 27.8 (3) NS ($P = 0.52$)	$P < 0.05$
KN-62 (10)	37.4 ± 3.7 (4) NS ($P = 0.11$)	61.1 ± 5.8 (5) $P < 0.01$	$P < 0.05$
ML-9 (30)	52.4 ± 6.9 (4) NS ($P = 0.70$)	95.9 ± 12.5 (3) NS ($P = 0.16$)	$P < 0.05$
Cerulenin (134)	49.2 ± 9.0 (4) NS ($P = 0.70$)	89.7 ± 3.8 (4) $P < 0.05$	$P < 0.05$

Exocytic events were counted between 0 and 15 s after the uncaging of NPE. Inhibitors were applied for 40 min, forskolin and 8-CPT-2'-*O*-Me-cAMP for 10 min, and 20 mM glucose for 1 min before UV irradiation. Data are means ± S.E.M. for the number of islets indicated in parentheses. The actions of the various compounds were compared first with the two-way Friedman test ($P < 0.001$), after which the Mann–Whitney *U* test was performed to compare values in the presence of test agent with the corresponding control or between 2.8 and 20 mM glucose, as indicated.

and of protein acylation in CIE with the use of specific inhibitors: bisindolylmaleimide I, KN-62, and ML-9, respectively, for the protein kinases and cerulenin for protein acylation (Yajima *et al.*, 2000; Straub *et al.*, 2002). None of these inhibitors significantly affected CIE in the presence of 2.8 mM glucose; although KN-62 and cerulenin inhibited CIE in the presence of 20 mM glucose, high glucose still had a significant facilitatory effect on CIE in the presence of these inhibitors (Table 3).

Control of the fusion pore by PKA

Finally, I probed the dynamics of the exocytic fusion pore by simultaneous imaging of two fluorescent tracers with different molecular sizes, SRB (~1.4 nm) and 10-kDa FD (~6 nm) (Takahashi *et al.*, 2002a). Insulin granules underwent full fusion in most (~93%) exocytic events during GIE (Fig. 6*A*), consistent with previous observations (Takahashi *et al.*, 2002a). Transient opening of the initial small pore, as revealed by staining with SRB but not with 10-kDa FD, was detected in 6.5% of events (Fig. 6*B*). The frequency of such transient opening was reduced to 3.8% in the presence of forskolin and increased to 10.3 or 9.8% in the presence of Rp-cAMPS or PKI (Table 4). These results suggested that PKA affects the fusion pore when its diameter is < 6 nm, and that the effects of the inhibitors on actual insulin secretion are slightly (~6%) larger than those presented in Table 1, since most insulin secretion occurs after the dilation of the pore larger than 12 nm (Takahashi *et al.*, 2002a).

The latency between the onset of staining of granules with SRB and that of their staining with 10-kDa FD (Fig. 6*A*), which reflects the dilation of the pore

from 1.4 to 6 nm, was not affected by forskolin, Rp-cAMPS, or PKI (Table 4). Moreover, none of these agents affected the time course of granule flattening, as reflected by the time ($T_{0.5}$) required for SRB fluorescence to decay to the half-maximal value (Fig. 6*C* and Table 4). These data suggested that cAMP does not affect the process of exocytosis after dilation of the fusion pore to > 6 nm.

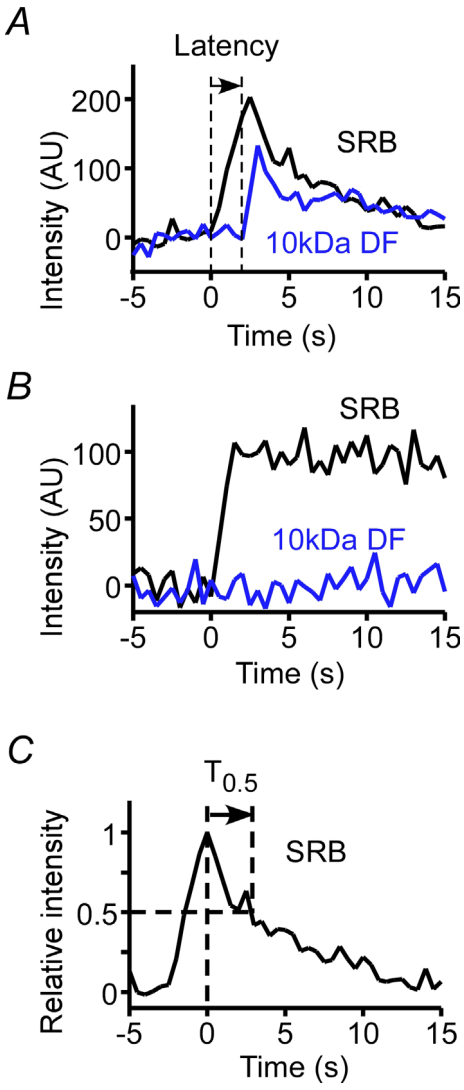

Figure 6. Opening of the fusion pore and full flattening of omega (Ω)–shaped exocytic profiles during GIE

A, typical example of a single exocytic event stained with both SRB and 10-kDa FD in an islet stimulated with 20 mM glucose. The latency between the onset of staining with SRB and that of staining with 10-kDa FD is indicated. AU, arbitrary units. *B*, example of transient opening of a small fusion pore, as revealed by staining of the event with SRB but not with 10-kDa FD. *C*, time course of flattening of an Ω-profile stained with SRB. The time ($T_{0.5}$) required for the fluorescence intensity to decrease to the half-maximal value is indicated.

Table 4. Fusion pore dynamics during GIE

Condition	Transient opening (%)	Latency (s)	$T_{0.5}$ (s)
Control	6.5 (367)	2.1 ± 0.1 (72)	2.8 ± 0.3 (137)
Forskolin (2 μM)	3.8* (447)	2.4 ± 0.1 (101)	3.0 ± 0.3 (196)
Rp-cAMPS (200 μM)	10.3* (311)	2.3 ± 0.1 (71)	3.2 ± 0.2 (133)
PKI (10 μM)	9.8 (82)	2.2 ± 0.1 (65)	2.7 ± 0.3 (71)

Islets were pretreated (or not) for 40 min with PKA inhibitors or for 10 min with forskolin and were then stimulated with 20 mM glucose. Transient opening of the fusion pore was identified as shown in Figure 6*B*. The latency between opening of the fusion pore to 1.4 nm and that to 6 nm was measured as shown in Figure 6*A*. The time of flattening of Ω-profiles ($T_{0.5}$) was measured as shown in Figure 6*C*. Latency and $T_{0.5}$ values are means ± S.E.M. The numbers of events for all data are indicated in parentheses. *P < 0.05 *versus* control (chi-square test).

Discussion

With the use of TEP imaging of pancreatic islets, I found that PKA antagonists markedly and selectively inhibited the initial period (~250 s) of the first phase (< 7 min) of GIE. These data suggest that the basal activity of PKA in islets is involved in glucose sensing during the initial period of GIE. The action of PKA was found not to be mediated by an effect on Ca^{2+} signaling, given that the PKA inhibitors did not affect glucose-induced increases in $[Ca^{2+}]_i$ under my experimental conditions. Consistently, glucose rapidly potentiated insulin exocytosis induced by the large increases in $[Ca^{2+}]_i$ generated by photolysis of a caged-Ca^{2+} compound (CIE) in a PKA dependent manner. This action of glucose was not mimicked by increases in the cytosolic concentration of cAMP, suggesting that the glucose action requires a cytosolic factor, which stimulates actions of PKA, and which is generated by glucose, but is not cAMP. Thus, PKA regulates insulin exocytosis in a glucose-dependent manner, and plays a major role in glucose sensing for insulin exocytosis, in addition to the role of the K_{ATP} channel-dependent mechanism.

Role of the basal activity of PKA in glucose-induced insulin exocytosis

Previous studies have shown that PKA inhibitors manifest relatively weak inhibitory (–25%) (Persaud *et al.*, 1990; Lester *et al.*, 1997) or insignificant (Harris *et al.*, 1997) effects on GIE. My data now suggest that the small effects of PKA inhibitors observed in these previous studies might be attributable to several factors. First, these studies relied on radioimmunoassay of insulin

secreted from islets during a period of 30–60 min; any effects of the antagonists on the first phase of GIE would thus likely have been masked. My imaging approach was able to evaluate effects of antagonists on insulin exocytosis with a time resolution of seconds and, consequently, was able to distinguish the first phase of insulin exocytosis from the second. Second, although H89 and KT5720 showed relatively weak effects in intact islets in the present study, my imaging approach revealed that their effects were much greater in small clusters of islet cells, suggesting that their ineffectiveness in whole islets was due to their poor penetration, as has previously been shown to be the case for lipophilic fluorescent tracers (Takahashi *et al.*, 2002b). Finally, I have shown that the effects of PKA inhibitors are dependent on the basal activity of PKA and may be less prominent in preparations in which this basal activity is suppressed, as is the case with the cluster preparations in the present study and with single β cells (Pipeleers *et al.*, 1985). Paracrine regulation, such as that mediated by glucagon secreted from α cells (Pipeleers *et al.*, 1985), might increase the basal activity of PKA in β cells present within intact islets. Furthermore, the PKA-dependent mechanism of glucose sensing might be expected to play a greater role *in vivo* than *in vitro*, given that the basal activity of PKA in β cells may also be increased by various hormones, such as incretins, present in the blood.

The PKA-dependent mechanism of glucose sensing

My finding that a high concentration of glucose enhanced CIE is consistent with the previous demonstration that high glucose facilitated insulin exocytosis induced by a high concentration of K^+ (Gembal *et al.*, 1992; Aizawa *et al.*, 1994).

These previous studies, however, investigated insulin secretion for longer time periods and under rather complex experimental conditions, in which K_{ATP} channels were activated with a channel agonist (diazoxide, 150–250 μM) and insulin secretion was triggered with high K^+ (20–50 mM), which induces spatially heterogeneous and moderate increases in $[Ca^{2+}]_i$ (Bokvist *et al.*, 1995). In contrast, I quantified CIE beginning 1 min after glucose application in cells subjected to large and spatially homogeneous increases in $[Ca^{2+}]_i$ in the absence of a K_{ATP} channel agonist. Despite the differences in experimental conditions, certain features of the facilitation by glucose were shared by the present and previous studies. First, forskolin was more effective in enhancing insulin exocytosis in the presence of high glucose (Gembal *et al.*, 1993; Yajima *et al.*, 1999). Second, inhibitors of conventional protein kinase C did not abrogate the glucose action (Sato & Henquin, 1998). Third, the action of glucose was rapid (Gembal *et al.*, 1992). And finally, ATP was implicated in the action of glucose (Detimary *et al.*, 1996; Sato & Henquin, 1998). It is thus possible that the two types of experiments revealed regulation of insulin exocytosis by the same underlying mechanism, whereas the results obtained with K_{ATP} channel agonist might also reflect the operation of slower processes activated by glucose, such as protein acylation (Yajima *et al.*, 2000; Straub *et al.*, 2002). My study has shown that PKA mediates the rapid effect of glucose on CIE, and that this action is operative during the initial period of the first phase of GIE.

The PKA-dependent mechanism does not constitutively regulate exocytosis. Indeed, increases in cytosolic concentrations of cAMP by forskolin

were not sufficient for the action of PKA on CIE, and a metabolite of glucose in the cytosol likely also be required. One candidate for such a metabolite is ATP, given that glucose induces a rapid increase in the cytosolic concentration of ATP (Henquin, 1990). Moreover, our research group has previously shown that the fast mode (mode 1) of CIE is augmented by cytosolic ATP in a concentration-dependent (0–5 mM) manner (Takahashi *et al.*, 1999; Kasai *et al.*, 2002) and that this effect requires both cAMP and PKA. Mode-1 exocytosis might thus account for the major part of the first phase of GIE (Fig. 7). An increase in the concentration of ATP can result in the activation of PKA in the absence of an increase in the concentration of cAMP (Takahashi *et al.*, 1999); such an effect might account for glucose action in the absence of cAMP accumulation (Gembal *et al.*, 1993; Yajima *et al.*, 1999).

The number of insulin vesicles responsible for mode-1 exocytosis is similarly estimated as ~22 events per cell both from GIE ([6.4 – 2.0] $cell^{-1}$ min^{-1} × 5 min; Table 1) and from CIE ([128.4 – 40.4] $cell^{-1}$ min^{-1} × 0.25 min; Table 3), assuming in the latter instance that the large increases in $[Ca^{2+}]_i$ rapidly triggered all available mode-1 exocytosis. In the presence of forskolin, however, the number was estimated as 59 events per cell from GIE ([13.8 – 2.0] × 5; Table 1), which is much greater than the value of 35 events per cell estimated from CIE ([182.5 – 40.4] × 0.25; Table 3). It is therefore possible that mode-1 vesicles are recruited when β cells experience a large increase in the cytosolic concentration of cAMP for > 2 min during GIE. Such a scenario may account for the fact that forskolin also augments the second phase of GIE (Takahashi *et al.*, 2002a) (Fig. 7). In the absence of forskolin, the second phase of GIE may

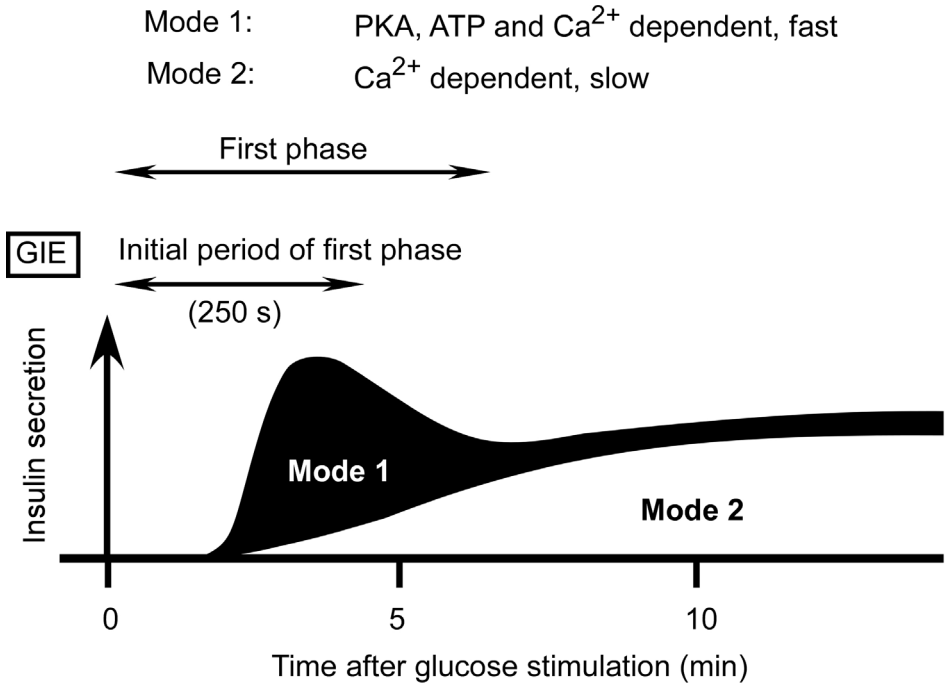

Figure 7. Scheme for the contribution of two distinct modes of exocytosis (modes 1 and 2) to the two phases of GIE

The initial period (250 s) of the first phase of GIE requires PKA. It is mediated mostly by mode-1 Ca^{2+}-dependent exocytosis, which is rapid and regulated by both PKA and ATP. Mode-1 exocytic vesicles may be recruited during glucose stimulation in the presence of a high cytosolic concentration of cAMP and can therefore also contribute to the later period of the first phase of GIE. The second phase of GIE is mediated predominantly by mode-2 Ca^{2+}-dependent exocytosis, which is slow and does not require PKA.

be mediated mostly by mode-2 exocytosis (Fig. 7), which is Ca^{2+} dependent but resistant to antagonists of cAMP and PKA and occurs more slowly than does mode-1 exocytosis (Takahashi *et al.*, 1999).

My observations that forskolin and inhibitors of PKA affected the fate of the fusion pore suggest that the action of PKA is mediated, at least in part, at the level of the fusion reaction. Several molecules are potential targets of PKA in this regard. One such candidate is SNAP25, a soluble *N*-ethylmaleimide-sensitive factor attachment protein receptor (SNARE); threonine-138 of this protein is phosphorylated by PKA (Nagy *et al.*, 2004) and is implicated in the early phase of Ca^{2+}-triggered exocytosis of large dense-core vesicles in chromaffin cells (Nagy *et al.*, 2004). Snapin, a protein that binds to SNARE complexes, is also a target of PKA in chromaffin cells (Chheda *et al.*, 2001); this protein is also expressed in β cells, but its role in exocytosis of large dense-core vesicles is unknown. Rab-interacting molecule-1 (RIM1) regulates neurotransmitter release at synapses and was shown to be a target of PKA (Lonart *et al.*, 2003); the phosphorylation site (serine-413) of this protein is also conserved in the related molecule RIM2 (Lonart *et al.*, 2003), which is expressed in β cells (Ozaki *et al.*, 2000; Kashima *et al.*, 2001).

In conclusion, I have shown that a PKA-dependent mechanism of glucose sensing operates during the initial period of the first phase of GIE. Impairment of the first phase of GIE has been implicated in the pathogenesis of type 2 diabetes (Ward *et al.*, 1984; Vaag *et al.*, 1995). In addition, the facilitatory effect of glucose on insulin secretion is defective in individuals with this disease (Ward *et al.*, 1984), with correction of this defect having been proposed as a new

strategy for diabetes treatment. Indeed, glucagon-like peptide-1 (GLP-1) and exendin, both of which are potential therapeutic agents for individuals with type 2 diabetes, have been found to activate PKA and to enhance insulin secretion in the presence of high plasma concentrations of glucose (Parkes *et al.*, 2001). Further elucidation of the molecular mechanism of PKA-dependent glucose sensing may provide new insight into the etiology of diabetes mellitus and lead to the development of novel therapies.

Acknowledgments

I’d like to extend my deepest thanks to Prof. Haruo Kasai (University of Tokyo) for continuous and valuable guidance, discussion, and encouragement throughout this research. Also, I’d like to express my sincere gratitude to Dr. Noriko Takahashi (University of Tokyo) for cooperation and helpful discussion throughout this research, Dr. Takuya Kishimoto (University of Tokyo) and Dr. Tomomi Nemoto (National Institute for Physiological Sciences) for many helpful suggestions. I thank Mr. Naoki Takahashi, Ms. Tamaki Kise, and Ms. Tokiko Suzuki for excellent technical assistance, and my friends and my family for kind support.

References

Aizawa T, Sato Y, Ishihara F, Taguchi N, Komatsu M, Suzuki N, Hashizume K, & Yamada T (1994). ATP-sensitive K^+ channel-independent glucose action in rat pancreatic beta-cell. *Am J Physiol* **266**, C622-C627.

Bennett BD, Jetton TL, Ying G, Magnuson MA, & Piston DW (1996). Quantitative subcellular imaging of glucose metabolism within intact pancreatic islets. *J Biol Chem* **271**, 3647-3651.

Bokvist K, Eliasson L, Ammala C, Renstrom E, & Rorsman P (1995). Co-localization of L-type Ca^{2+} channels and insulin-containing secretory granules and its significance for the initiation of exocytosis in mouse pancreatic B-cells. *EMBO J* **14**, 50-57.

Bugrim AE (1999). Regulation of Ca^{2+} release by cAMP-dependent protein kinase. A mechanism for agonist-specific calcium signaling? *Cell Calcium* **25**, 219-226.

Chheda MG, Ashery U, Thakur P, Rettig J, & Sheng ZH (2001). Phosphorylation of Snapin by PKA modulates its interaction with the SNARE complex. *Nat Cell Biol* **3**, 331-338.

Detimary P, Van den BG, & Henquin JC (1996). Concentration dependence and time course of the effects of glucose on adenine and guanine nucleotides in mouse pancreatic islets. *J Biol Chem* **271**, 20559-20565.

Dyachok O & Gylfe E (2004). Ca^{2+}-induced Ca^{2+} release via inositol 1,4,5-trisphosphate receptors is amplified by protein kinase A and triggers exocytosis in pancreatic beta-cells. *J Biol Chem* **279**, 45455-45461.

Enserink JM, Christensen AE, de Rooij J, van Triest M, Schwede F, Genieser HG, Doskeland SO, Blank JL, & Bos JL (2002). A novel Epac-specific cAMP

analogue demonstrates independent regulation of Rap1 and ERK. *Nat Cell Biol* **4**, 901-906.

Eto K, Tsubamoto Y, Terauchi Y, Sugiyama T, Kishimoto T, Takahashi N, Yamauchi N, Kubota N, Murayama S, Aizawa T, Akanuma Y, Aizawa S, Kasai H, Yazaki Y, & Kadowaki T (1999). Role of NADH shuttle system in glucose-induced activation of mitochondrial metabolism and insulin secretion. *Science* **283**, 981-985.

Fournier L, Whitfield JF, Schwartz JL, & Begin-Heick N (1994). Cyclic AMP triggers large $[Ca^{2+}]_i$ oscillations in glucose-stimulated beta-cells from ob/ob mice. *J Biol Chem* **269**, 1120-1124.

Fujita-Yoshigaki J, Dohke Y, Hara-Yokoyama M, Furuyama S, & Sugiya H (1999). Presence of a complex containing vesicle-associated membrane protein 2 in rat parotid acinar cells and its disassembly upon activation of cAMP-dependent protein kinase. *J Biol Chem* **274**, 23642-23646.

Gembal M, Detimary P, Gilon P, Gao ZY, & Henquin JC (1993). Mechanisms by which glucose can control insulin release independently from its action on adenosine triphosphate-sensitive K^+ channels in mouse B cells. *J Clin Invest* **91**, 871-880.

Gembal M, Gilon P, & Henquin JC (1992). Evidence that glucose can control insulin release independently from its action on ATP-sensitive K^+ channels in mouse B cells. *J Clin Invest* **89**, 1288-1295.

Grapengiesser E, Gylfe E, & Hellman B (1991). Cyclic AMP as a determinant for glucose induction of fast Ca^{2+} oscillations in isolated pancreatic beta-cells. *J Biol Chem* **266**, 12207-12210.

Harris TE, Persaud SJ, & Jones PM (1997). Pseudosubstrate inhibition of cyclic AMP-dependent protein kinase in intact pancreatic islets: effects on cyclic AMP-dependent and glucose-dependent insulin secretion. *Biochem Biophys*

Res Commun **232**, 648-651.

Henquin JC (1990). Cellular mechanisms of the control of insulin secretion. *Arch Int Physiol Biochim* **98**, A61-A80.

Hilfiker S, Czernik AJ, Greengard P, & Augustine GJ (2001). Tonically active protein kinase A regulates neurotransmitter release at the squid giant synapse. *J Physiol* **531**, 141-146.

Hill RS, Oberwetter JM, & Boyd AE, III (1987). Increase in cAMP levels in beta-cell line potentiates insulin secretion without altering cytosolic free-calcium concentration. *Diabetes* **36**, 440-446.

Hutton JC (1989). The insulin secretory granule. *Diabetologia* **32**, 271-281.

Ito K, Miyashita Y, & Kasai H (1999). Kinetic control of multiple forms of Ca^{2+} spikes by inositol trisphosphate in pancreatic acinar cells. *J Cell Biol* **146**, 405-413.

Kaneko M & Takahashi T (2004). Presynaptic mechanism underlying cAMP-dependent synaptic potentiation. *J Neurosci* **24**, 5202-5208.

Kang G, Chepurny OG, Rindler MJ, Collis L, Chepurny Z, Li WH, Harbeck M, Roe MW, & Holz GG (2005). A cAMP and Ca^{2+} coincidence detector in support of Ca^{2+}-induced Ca^{2+} release in mouse pancreatic beta cells. *J Physiol* **566**, 173-188.

Kasai H, Hatakeyama H, Kishimoto T, Liu T-T, Nemoto T, & Takahashi N (2005). A new quantitative (two-photon extracellular polar-tracer imaging-based quantification (TEPIQ)) analysis for diameters of exocytic vesicles and its application to pancreatic islets. *J Physiol* **568**, 891-903.

Kasai H, Suzuki T, Liu TT, Kishimoto T, & Takahashi N (2002). Fast and cAMP-sensitive mode of Ca^{2+}-dependent exocytosis in pancreatic beta-cells.

Diabetes **51 Suppl 1**, S19-S24.

Kashima Y, Miki T, Shibasaki T, Ozaki N, Miyazaki M, Yano H, & Seino S (2001). Critical role of cAMP-GEFII-Rim2 complex in incretin-potentiated insulin secretion. *J Biol Chem* **276**, 46046-46053.

Kishimoto T, Liu T-T, Hatakeyama H, Nemoto T, Takahashi N, & Kasai H (2005). Sequential compound exocytosis of large dense-core vesicles in PC12 cells studied with TEPIQ (two-photon extracellular polar-tracer imaging-based quantification) analysis. *J Physiol* **568**, 905-915.

Lester LB, Langeberg LK, & Scott JD (1997). Anchoring of protein kinase A facilitates hormone-mediated insulin secretion. *Proc Natl Acad Sci U S A* **94**, 14942-14947.

Liu T-T, Kishimoto T, Hatakeyama H, Nemoto T, Takahashi N, & Kasai H (2005). Exocytosis and endocytosis of small vesicles in PC12 cells studied with TEPIQ (two-photon extracellular polar-tracer imaging-based quantification) analysis. *J Physiol* **568**, 917-929.

Lonart G, Schoch S, Kaeser PS, Larkin CJ, Sudhof TC, & Linden DJ (2003). Phosphorylation of RIM1a by PKA triggers presynaptic long-term potentiation at cerebellar parallel fiber synapses. *Cell* **115**, 49-60.

Marie JC & Bailbe D (2000). Cytosolic calcium handling in islets of normal Wistar and diabetic Goto Kakizaki rats in the presence of glucose and truncated glucagon-like peptide 1 (7-36) amide. *Ann N Y Acad Sci* **921**, 464-468.

Matthies H & Reymann KG (1993). Protein kinase A inhibitors prevent the maintenance of hippocampal long-term potentiation. *Neuroreport* **4**, 712-714.

Nagy G, Reim K, Matti U, Brose N, Binz T, Rettig J, Neher E, & Sorensen JB (2004). Regulation of releasable vesicle pool sizes by protein kinase A-dependent phosphorylation of SNAP-25. *Neuron* **41**, 417-429.

Nemoto T, Kimura R, Ito K, Tachikawa A, Miyashita Y, Iino M, & Kasai H (2001). Sequential-replenishment mechanism of exocytosis in pancreatic acini. *Nat Cell Biol* **3**, 253-258.

Nesher R & Cerasi E (2002). Modeling phasic insulin release: immediate and time-dependent effects of glucose. *Diabetes* **51 Suppl 1**, S53-S59.

Ozaki N, Shibasaki T, Kashima Y, Miki T, Takahashi K, Ueno H, Sunaga Y, Yano H, Matsuura Y, Iwanaga T, Takai Y, & Seino S (2000). cAMP-GEFII is a direct target of cAMP in regulated exocytosis. *Nat Cell Biol* **2**, 805-811.

Parkes DG, Pittner R, Jodka C, Smith P, & Young A (2001). Insulinotropic actions of exendin-4 and glucagon-like peptide-1 in vivo and in vitro. *Metabolism* **50**, 583-589.

Persaud SJ, Jones PM, & Howell SL (1990). Glucose-stimulated insulin secretion is not dependent on activation of protein kinase A. *Biochem Biophys Res Commun* **173**, 833-839.

Pipeleers DG, Schuit FC, in't Veld PA, Maes E, Hooghe-Peters EL, Van de WM, & Gepts W (1985). Interplay of nutrients and hormones in the regulation of insulin release. *Endocrinology* **117**, 824-833.

Porterfield DM, Corkey RF, Sanger RH, Tornheim K, Smith PJ, & Corkey BE (2000). Oxygen consumption oscillates in single clonal pancreatic beta-cells (HIT). *Diabetes* **49**, 1511-1516.

Renstrom E, Eliasson L, & Rorsman P (1997). Protein kinase A-dependent and -independent stimulation of exocytosis by cAMP in mouse pancreatic B-cells. *J Physiol* **502 (Pt 1)**, 105-118.

Rorsman P & Abrahamsson H (1985). Cyclic AMP potentiates glucose-induced insulin release from mouse pancreatic islets without increasing cytosolic free Ca^{2+}. *Acta Physiol Scand* **125**, 639-647.

Sakaba T & Neher E (2003). Direct modulation of synaptic vesicle priming by $GABA_B$ receptor activation at a glutamatergic synapse. *Nature* **424**, 775-778.

Sato K, Ohsaga A, Oshiro T, Ito S, & Maruyama Y (2002). Involvement of GTP-binding protein in pancreatic cAMP-mediated exocytosis. *Pflugers Arch* **443**, 394-398.

Sato Y & Henquin JC (1998). The K^+-ATP channel-independent pathway of regulation of insulin secretion by glucose: in search of the underlying mechanism. *Diabetes* **47**, 1713-1721.

Straub SG, Yajima H, Komatsu M, Aizawa T, & Sharp GW (2002). The effects of cerulenin, an inhibitor of protein acylation, on the two phases of glucose-stimulated insulin secretion. *Diabetes* **51 Suppl 1**, S91-S95.

Takahashi N, Hatakeyama H, Okado H, Miwa A, Kishimoto T, Kojima T, Abe T, & Kasai H (2004). Sequential exocytosis of insulin granules is associated with redistribution of SNAP25. *J Cell Biol* **165**, 255-262.

Takahashi N, Kadowaki T, Yazaki Y, Ellis-Davies GC, Miyashita Y, & Kasai H (1999). Post-priming actions of ATP on Ca^{2+}-dependent exocytosis in pancreatic beta cells. *Proc Natl Acad Sci U S A* **96**, 760-765.

Takahashi N, Kadowaki T, Yazaki Y, Miyashita Y, & Kasai H (1997). Multiple exocytotic pathways in pancreatic beta cells. *J Cell Biol* **138**, 55-64.

Takahashi N, Kishimoto T, Nemoto T, Kadowaki T, & Kasai H (2002a). Fusion pore dynamics and insulin granule exocytosis in the pancreatic islet. *Science* **297**, 1349-1352.

Takahashi N, Nemoto T, Kimura R, Tachikawa A, Miwa A, Okado H, Miyashita Y, Iino M, Kadowaki T, & Kasai H (2002b). Two-photon excitation imaging of pancreatic islets with various fluorescent probes. *Diabetes* **51 Suppl 1**, S25-S28.

Trudeau LE, Emery DG, & Haydon PG (1996). Direct modulation of the secretory machinery underlies PKA-dependent synaptic facilitation in hippocampal neurons. *Neuron* **17**, 789-797.

Vaag A, Henriksen JE, Madsbad S, Holm N, & Beck-Nielsen H (1995). Insulin secretion, insulin action, and hepatic glucose production in identical twins discordant for non-insulin-dependent diabetes mellitus. *J Clin Invest* **95**, 690-698.

Ward WK, Bolgiano DC, McKnight B, Halter JB, & Porte D, Jr. (1984). Diminished B cell secretory capacity in patients with noninsulin-dependent diabetes mellitus. *J Clin Invest* **74**, 1318-1328.

Wokosin DL, Loughrey CM, & Smith GL (2004). Characterization of a range of fura dyes with two-photon excitation. *Biophys J* **86**, 1726-1738.

Wollheim CB & Sharp GW (1981). Regulation of insulin release by calcium. *Physiol Rev* **61**, 914-973.

Yada T, Itoh K, & Nakata M (1993). Glucagon-like peptide-1-(7-36)amide and a rise in cyclic adenosine 3',5'-monophosphate increase cytosolic free Ca^{2+} in rat pancreatic beta-cells by enhancing Ca^{2+} channel activity. *Endocrinology* **133**, 1685-1692.

Yaekura K, Kakei M, & Yada T (1996). cAMP-signaling pathway acts in selective synergism with glucose or tolbutamide to increase cytosolic Ca^{2+} in rat pancreatic beta-cells. *Diabetes* **45**, 295-301.

Yaekura K & Yada T (1998). $[Ca^{2+}]_i$-reducing action of cAMP in rat pancreatic beta-cells: involvement of thapsigargin-sensitive stores. *Am J Physiol* **274**, C513-C521.

Yajima H, Komatsu M, Schermerhorn T, Aizawa T, Kaneko T, Nagai M, Sharp GW, & Hashizume K (1999). cAMP enhances insulin secretion by an action on

the ATP-sensitive K^+ channel-independent pathway of glucose signaling in rat pancreatic islets. *Diabetes* **48**, 1006-1012.

Yajima H, Komatsu M, Yamada S, Straub SG, Kaneko T, Sato Y, Yamauchi K, Hashizume K, Sharp GW, & Aizawa T (2000). Cerulenin, an inhibitor of protein acylation, selectively attenuates nutrient stimulation of insulin release: a study in rat pancreatic islets. *Diabetes* **49**, 712-717.